MOX–Report No. 16/2012

Drug delivery patterns for different stenting techniques in coronary bifurcations: a comparative computational study

Cutr, E.; Zunino, P.; Morlacchi, S.; Chiastra, C.; Migliavacca, F.

MOX, Dipartimento di Matematica "F. Brioschi"
Politecnico di Milano, Via Bonardi 9 - 20133 Milano (Italy)

mox@mate.polimi.it http://mox.polimi.it

Drug delivery patterns for different stenting techniques in coronary bifurcations: a comparative computational study

Elena Cutrì[1], Paolo Zunino[1,2,*], Stefano Morlacchi[3,4],
Claudio Chiastra[3,4], Francesco Migliavacca[3]

[1] Modelling and Scientific Computing (MOX), Department of Mathematics, Politecnico di Milano, Milan, Italy
[2] Department of Mechanical Engineering and Materials Science, University of Pittsburgh, PA, USA
[3] Laboratory of Biological Structure Mechanics (LaBS), Structural Engineering Department, Politecnico di Milano, Milan, Italy
[4] Bioengineering Department, Politecnico di Milano, Milan, Italy

Keywords: drug eluting stents, finite element analysis, computational fluid dynamics, stenting techniques

Abstract

The treatment of coronary bifurcation lesions represents a challenge for the interventional cardiologists due to the lower rate of procedural success and the higher risk of restenosis. The advent of drug eluting stents (DES) has dramatically reduced restenosis and consequently the request for re-intervention. The aim of the present work is to provide further insight about the effectiveness of DES by means of a computational study that combines virtual stent implantation, fluid dynamics and drug release for different stenting protocols currently used in the treatment of a coronary artery bifurcation. An explicit dynamic finite element model is developed in order to obtain realistic configurations of the implanted devices used to perform fluid dynamics analysis by means of a previously developed finite element method coupling the blood flow and the intramural plasma filtration in rigid arteries. To efficiently model the drug release, a multiscale strategy is adopted, ranging from lumped parameter model accounting for drug release, to fully 3-D models for drug transport to the artery. Differences in drug delivery to the artery are evaluated with respect to local drug dosage. This model allowed to compare alternative stenting configurations (namely, the Provisional Side Branch, the Culotte and the Inverted Culotte techniques), thus suggesting guidelines in the treatment of coronary bifurcations lesions and addressing clinical issues such as the effectiveness of drug delivery to lesions in the side branch, as well as the influence of incomplete strut apposition and overlapping stents.

Introduction

The treatment of coronary bifurcation lesions occurs up to 16% of coronary treatments [1,2] and represents a major challenge for interventional cardiologists due to a lower rate of procedural success and a higher risk of restenosis.
Before the advent of stents, these lesions were treated using balloon angioplasty. The main limitations of such treatment were the plaque shift that could lead to lateral vessel occlusion and the acute elastic recoil of the vessel wall. The final kissing balloon (FKB) dilatation, consisting in the simultaneous

* corresponding author: Tel +1 412 624 9774
Fax +1 412 624 4846
Email paz13@pitt.edu

balloon expansion in both the main branch (MB) and the side branch (SB) allowed to overcome the plaque shift, but the elastic recoil of the vessel still remains an unsolved problem.
Bare metal stents (BMS) were designed to scaffold the arterial wall avoiding the acute vessel closure. Nevertheless, the development of neointimal hyperplasia, occurring after BMS implantation, impairs the performance of the device and results in long term in-stent restenosis. The choice of the most convenient technique for stenting bifurcations is controversial. On the one hand, studies on BMS [3,4] showed that a two stents procedure was associated to a higher rate of restenosis with respect to the single stent procedures and a longer interventional time [5]. On the other hand, implantation of only one stent in the MB may compromise the flow in the SB through a combination of plaque shift and "pinching" by the stent struts [5].
The advent of drug eluting stents (DES) in the treatment of coronary artery diseases has dramatically reduced in-stent restenosis and consequently the request for re-intervention [6]. As suggested in Park et al. [7], the previous indications on stenting techniques performed using BMS should be reinterpreted in the DES era. In particular, stent pattern, strut geometry, interactions with luminal flow, arterial tissue transport and uptake properties are expected to significantly affect arterial drug distribution, which is hardly evaluated by means of experimental techniques.
Several computational models have been recently proposed to analyze drug release in the arteries using one-dimensional [8,9], bi-dimensional [10-13], or three-dimensional approaches. These 3-D models consist of either using a simplified geometry [14] or deriving it from the simulations of stent expansion [15,16]. The arterial wall is generally modeled as a homogenous porous medium, including drug advection due to plasma leakage. In addition to this model setting, some authors account for drug binding to tissue proteins, others include anisotropic drug diffusivity or the presence of atherosclerotic plaque. Other studies [17-22] are focused on local hemodynamics neglecting anisotropic diffusion, coating and tissue porosity, plasma filtration in the tissue, and protein effects.
The aim of the present work is to provide further insight on the effectiveness of DES by means of computational analyses that combine virtual stent implantation, fluid dynamics and drug release for three different procedures (Provisional [1], Culotte [23,24] and Inverted Culotte [25]) used in the treatment of a coronary artery bifurcation. First, an explicit dynamic structural finite element model is implemented to obtain realistic configurations of the implanted device. Then, fluid dynamics is achieved by means of a previously developed [26,27] finite element method coupling the blood flow and intramural plasma filtration in rigid arteries. In particular, the former is described using Navier-Stokes equations and the latter is addressed by means of the Darcy law. Finally, to efficiently model the drug release, a multiscale strategy is adopted, ranging from lumped parameter models, accounting for drug release to fully 3-D models for drug transport to the artery [28] (Fig. 1).

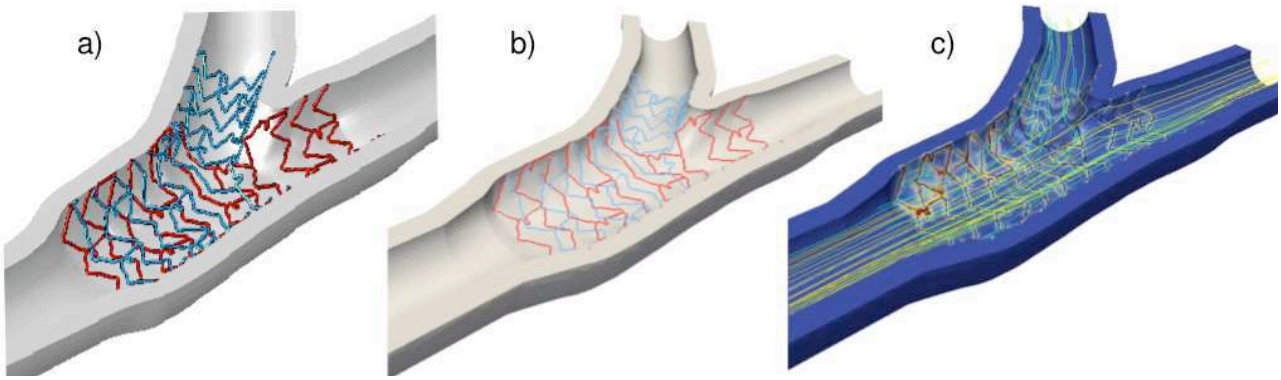

Figure 1: Computational model of DES: a) 3D geometry of the DESs implanted in the coronary bifurcation via a structural finite element model; b) 1D model of DESs built form the 3D geometry; c) drug concentration in the arterial wall (blue to red code), blood velocity in the arterial lumen (streamlines) and 1D geometry of the two DESs.

Differences in drug delivery to the artery in the MB and in the SB are evaluated, thus suggesting guidelines in the treatment of coronary bifurcations lesions. The proposed model might be useful to address clinical issues such as the effectiveness in the treatment of lesions in the SB, the influence of incomplete strut apposition and stent overlap on drug delivery.

Materials and Methods

A computational model for DES

Two consecutive modeling phases are carried out: in the former the stents are expanded into the bifurcated coronary artery by means of structural simulation performed with ABAQUS/Explicit commercial code (Dassault Systèmes Simulia Corporation, RI, USA); in the latter, starting from this deformed configuration, the analysis of fluid dynamics and drug release is performed with an in-house code [26,27].

Phase I: Realistic structural model of a stented artery

A model of coronary bifurcation is created with an angle of 45°, a thickness of the arterial wall of 0.9 mm and internal diameters of the MB and SB equal to 2.78 and 2.44 mm, respectively.

The geometry of the investigated stents resembles two commercial devices: the standard Multilink Vision (Abbott Laboratories, Abbott Park, IL; USA) and Tryton (Tryton Medical Inc, Durham, NC, USA), a new dedicated BMS for coronary bifurcations.

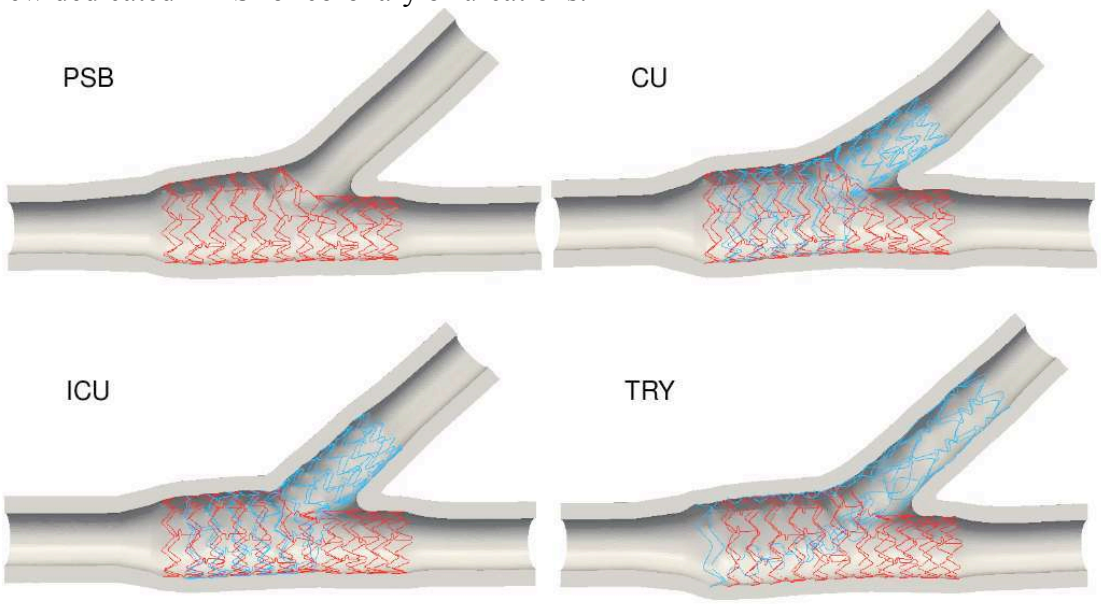

Figure 2: Coronary bifurcations after stents implantation using provisional side branch (PSB), culotte (CU) and Inverted Culotte (ICU) techniques, and Inverted Culotte (ICU) technique with Tryton stent (TRY).

Three different stenting procedures are simulated using the Multilink stent model: the Provisional Side Branch (PSB), the Culotte (CU) and the Inverted Culotte (ICU) (Fig. 2). The PSB is a one-stent technique that consists in the implantation of a stent in the MB across the bifurcation followed by a FKB inflation that allows to free the SB access from stent struts. The CU is a two-stent technique in which, after a PSB stenting, another stent is inserted in the SB. The procedure is ended with the FKB inflation. The third case investigated is the ICU technique consisting in the expansion of a stent in the SB followed by the implantation of the second stent in the MB and finally concluded by FKB inflation. The main drawback of the two Culotte techniques is the wide overlap region of the two implanted

devices resulting in a double metallic layer in the proximal part of the MB. To overcome this limitation, a new ICU approach, where Tryton is implanted as a SB stent, has been proposed in clinical literature and hereby investigated (TRY), too.
In order to reach realistic geometrical configurations, the stented bifurcation model is obtained running structural analysis by means of ABAQUS/Explicit with the method developed in Gastaldi et al. [29]. Then, the final configurations are exported as triangulated surfaces and used to create the fluid domains for the subsequent analyses [30].

Phase II: Fluid dynamics and drug release
Drug release, transport in the blood stream and absorption into the arterial wall are described by the model developed in [28] and briefly summarized below. Quantities related to the stent are denoted with (s), the ones related to the arterial lumen and wall are labeled by (l) and (w), respectively. The model takes into account diffusion and dissolution mediated drug release process with finite dissolution rate according to the equations proposed in [31]. Starting from an initial solid concentration, drug dissolves and diffuses through the interstices of the DES coating in order to finally reach the outer surface and be released. The solution of such equation is analytically approximated by means of asymptotic expansions and the profile of the drug release rate $J_s(t,x)$ is explicitly quantified in [32] as

$$J_s(t,x) = -(1-a(t,x)erf(\Gamma)^{-1}\sqrt{\frac{D_s}{\pi t}})$$

where Γ is a correction coefficient depending on the substrate physical properties and $a(t,x)$ denotes the drug concentration into the artery (referring either to the lumen or the wall). Drug concentrations are non-dimensional values referred to the saturation level of dissolved drug in water, $\bar{c}$, which assumes the unit value. For advection and diffusion of released drug in the blood steam, blood is modeled as a Newtonian fluid subject to Navier-Stokes equations complemented by steady boundary conditions, as in [26,33,34]. In particular, we impose a steady parabolic velocity profile whose peak reaches 240mm/s at the inflow of the vascular district and 70/30 flow division between the MB and SB respectively at the outflow[35]. Such conditions correspond to a physiological coronary mean flow rate over a heartbeat. The drug concentration inside the lumen, a_l, is governed by an advection, diffusion model:

$$\partial_t a_l - \nabla(D_l \nabla a_l) + u \cdot \nabla a_l + 2\pi R_s \zeta_l(x) J_s(t,x) \delta_s(x) = 0$$

where the novelty consists in considering the DES as a concentrated drug source represented by the term $2\pi R_s \zeta_l(x) J_s(t,x) \delta_s(x)$, featuring a Dirac mass $\delta_s(x)$ located on the meanline of DES struts and modulated by the local intensity of drug release $J_s(t,x)$ multiplied by the strut section perimeter $2\pi R_s$ with assumption of circular shape. The effective radius R_s is computed to make sure that the effective release surface is equivalent to the real one. Assuming that the real struts feature a rectangular section with perimeter P, the radius is given by $R_s = P/2\pi$. The factor $0 \le \zeta_l(x) \le 1$ quantifies the fraction of the stent surface embedded in the lumen. Drug absorption into the arterial wall is described by means of a system of similar equations including dynamic binding of the drug to the extracellular matrix [36,37]. The free drug concentration a_w and density of free binding sites b_w in the arterial wall are respectively governed by

$$\partial_t a_w - \partial_t b_w - \nabla(D_w \nabla a_w) + u \cdot \nabla a_w + 2\pi R_s \zeta_w(x) J_s(t,x) \delta_s(x) = 0 \text{ with } \zeta_w(x) = 1 - \zeta_l(x)$$

$$\partial_t b_w + k_{on} a_w b_w + k_{off}(b_w - b_{w,0}) = 0$$

Initial and inflow drug concentrations, as well as outflow diffusion fluxes are set to zero. At the interface between the lumen and the arterial wall, continuity of drug concentration and fluxes is enforced, to satisfy mass conservation between the two regions. Intramural plasma filtration promoted by the pressure drop form the inner to the outer surface of the artery convects the drug through the arterial wall. This flow is modeled by means of the Darcy law of filtration and computational studies performed in [26] suggest that physiological arterial leakage affects the release profile promoting a deeper penetration of drug in the artery and a quicker washout.
The drug release and absorption model is complemented with coefficients corresponding to release of heparin and for this molecule validation of the release rate $J_s(t,x)$ has been performed in [28] by comparison with the classical Higuchi model [38]. According to [39] we set the diffusivity of the drug in the arterial tissue to $D_w = 7.7 \times 10^{-6}\, mm^2/s$ and the diffusivity in the lumen to $D_l = 1.5 \times 10^{-4}\, mm^2/s$. As regards the ligand/receptor interaction involving drug and proteins contributing to form the tissue extracellular matrix, we apply data from [37] where the binding reaction constants are $k_{on} = 10^2 s^{-1}$ and $k_{off} = 10^{-2} s^{-1}$ and the average concentration of receptors in the tissue is set to $b_{w,0} = 5$ (we recall that all data refer to non-dimensional concentrations). For the stent struts we assume a squared section 0.08 mm wide (which is coherent with the selected stent platform, see [40]). As a result of that, the equivalent radius is $R_s = 0.052mm$. The coating consists of a polymeric film $L = 7\mu m$ thick. We assume that the initial drug charge, c_s, is 10 times the drug saturation level in water, namely $c_s = 10\bar{c}$. According to the model developed in [28,32], the value of c_s determines the coefficient Γ that in this case is equal to 0.23. A reasonable value for heparin diffusivity in polymers (in particular aliphatic polyesters such as poly-lactic or poly-glycolic acids) is $D_s = 10^{-8}\, mm^2/s$, also confirmed by [37]. These data correspond to a fast release profile; indeed, according to an estimate provided in [28,32], after $T = L^2/(4D_s\Gamma^2) = 6h21'$ about 95% of the available drug has been released. As a consequence, the final time of the computational simulations for drug release is set to T. If the drug chemical formula or coating material are modified, drug diffusivity, release rate and consequently the release profile can vary over several orders of magnitude. However, since this study has a comparative nature, the conclusions of this work are substantially insensitive with respect to the release profile.

Design of Experiments
The DES model is used to compare different configurations when varying the stenting technique among PSB, CU or ICU options. Regarding the Culotte techniques, both configurations with one (-MB and -SB) and two (-MBSB) stents releasing drug are analyzed.
The systematic combination of these two factors gives rise to 7 significant tests, which are labeled as Test PSB-MB (PSB, MB active), Test CU-MB (Culotte, MB active), Test ICU-MB (ICU, MB active), Test CU-SB (Culotte, SB active), Test ICU-SB (ICU, SB active), Test CU-MBSB (Culotte, MB+SB active), Test ICU-MBSB (ICU, MB+SB active). The simultaneous comparison of all cases will suggest guidelines to select what stenting procedure provides an optimal distribution of drug in regions at risk of restenosis, without reaching toxic drug concentrations. In addition, we also compare these cases,

which coherently refer to the same Multilink Vision DES platform, with the Tryton platform [41], specifically developed for the treatment of bifurcations and labeled as Test TRY-MB in the forthcoming analysis. For this case, stents are implanted by means of the ICU technique and drug elution is activated for the MB stent only.

The main feature characterizing the present model with respect to other examples proposed in literature is the ability to handle fully realistic stent geometries with moderate computational effort. Since the stent is accounted by means of its mean line solely and it is completely independent from the other components of the geometrical model, we can easily manipulate the stent pattern without affecting the computational mesh for approximating fluid dynamics and mass transport. Such feature of the model helps us to quantify the losses of released drug due to strut superposition in case of two-stent techniques, which is a significant issue to be addressed, as highlighted in Kolachalama et al. [33]. This task is achieved by complementing each test case with an idealized one, where only the configuration of the struts is slightly modified to perfectly adhere to the arterial wall. The results of drug release for such idealized configuration are systematically compared to the realistic one obtained by finite element analysis of stent expansion. In such a way, we are able to isolate the influence of incomplete strut apposition to the arterial wall from other factors affecting drug uptake.

Quantities of interest

Local concentration profiles inside the arterial wall are the results of the numerical simulations. However, such large datasets do not seem to be very helpful to analyze DES efficacy and driving conclusions. In alternative, we consider averaged data such as drug dose, which is the time-averaged drug concentration at each point of the arterial wall and its mean value on a portion (V) of the artery. More precisely, given the distribution of free $(a_w(t,x))$ and bound drug $(b_{w,0}-b_w(t,x))$ in a control volume (V), we denote by $c_w(t,x)=a_w(t,x)+b_{w,0}-b_w(t,x)$ the total drug concentration. The drug delivered to V at time t is $M(c_w,V,t)=\int_V c_w(t,x)\,dV$ and the corresponding mean value is $\bar{c}_w(V,t)=V^{-1}M(c_w,V,t)$. Drug dose is a scalar field defined by $d_w(x)=T^{-1}\int_0^T c_w(t,x)\,dt$ and its mean value is $\bar{d}_w(V)=V^{-1}M(d_w,V)$. Also the maximum dose $d_w^{\max}(V)=\max_{x\in V} d_w(x)$ is addressed. Concerning the definition of V, beside the entire arterial wall (denoted with V_{TOT} in Figure 3), we analyze drug delivery to three specific regions (see Figure 3), namely the proximal part of the MB with respect to the bifurcation (denoted with V_{MBP}), the distal part of the MB (denoted with V_{MBD}) and the central part of the side branch (denoted with V_{SB}).

Figure 3: Regions V_{TOT}, V_{MBP}, V_{MBD}, V_{SB} depicted from left to right, respectively.

In order to compare different delivery systems under normalized conditions with respect to active surface for drug delivery, diffusion properties of the substrate matrix and time scales, a non-

dimensional drug delivery indicator is also introduced. To this purpose, for each delivery system we define a reference amount of deliverable drug within a time interval $(0,T)$, quantified by $M_{ref}(V) = c_s A_{ref}(V)\sqrt{D_s \cdot T}$ where $c_s = 10\bar{c}$ is DES nominal drug charge, $A_{ref}(V)$ is the DES active surface in V and D_s is the diffusion coefficient in the coating releasing the drug. Then, $M_{eff} = M(V,t)\big/ M_{ref}(V)$ represents a normalized amount of delivered drug and it is independent of the release rate and of the active stent surface. The comparison of this quantity for different stenting configurations provides information on the effectiveness of drug delivery. Finally, it should be noticed that in all the aforementioned tests the quantity $M(V,t)$ evolves with time as $\sqrt{t}$, because the release rate $J_s(t,x)$ is proportional to $1/\sqrt{t}$. Since $\sqrt{t}$ is monotonically increasing, it is sufficient to analyze the amount of drug released at the final time T to characterize the entire release history.

Results and Discussion

The results of the computational DES model are reported in Figures 4, 5, 6, 7 in terms of $d_w(x)$, $c_w(t,x)$, $d_w^{\max}(V)$, M_{eff}, respectively. Note that scales for the panels V_{TOT} and V_{MBP} are different from those in V_{MBD} and V_{SB}.

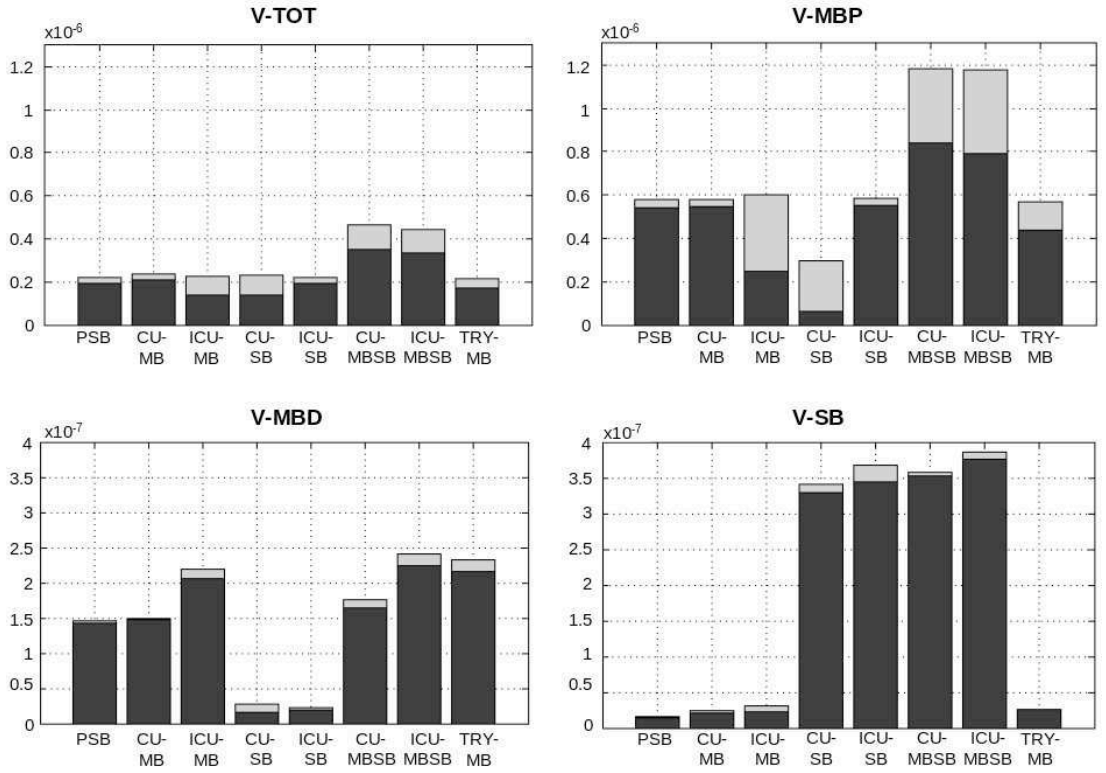

FIGURE 4: the mean value of the dose, namely $\bar{d}_w(V) = V^{-1}M(d_w,V)$, quantified over the regions V_{TOT}, V_{MBP}, V_{MBD} and V_{SB} from left to right, top to bottom.

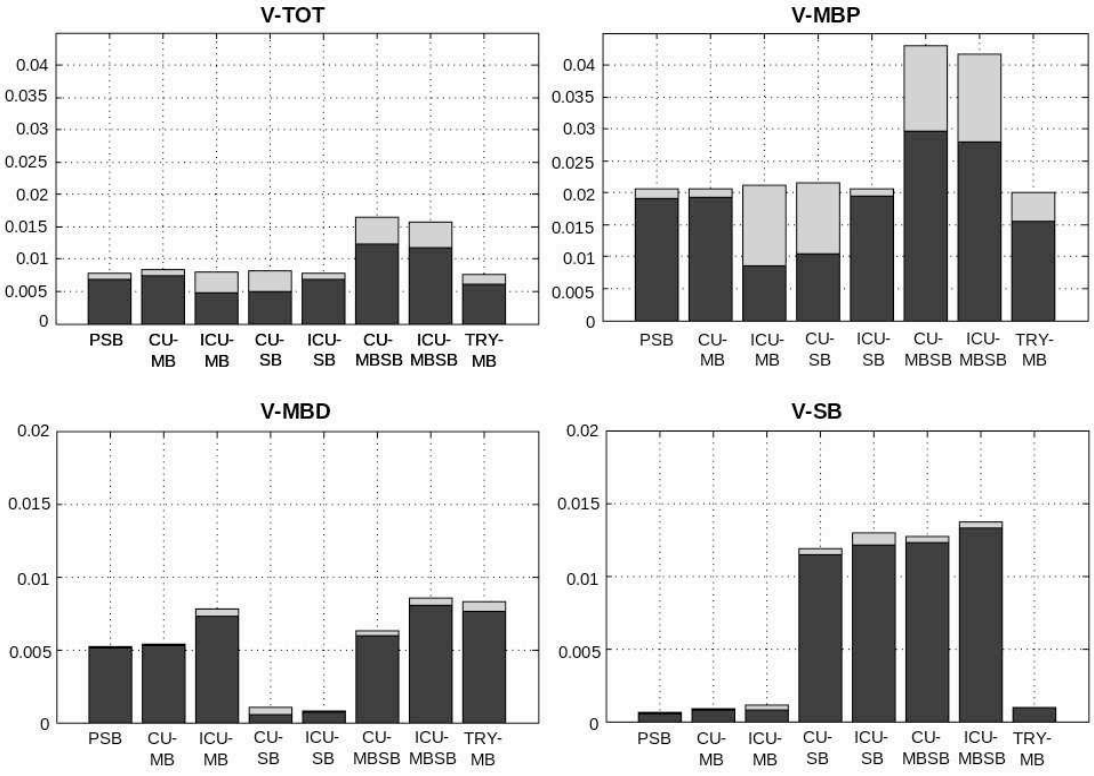

FIGURE 5: the mean value of the total drug concentration evaluated at final release time T, namely $\bar{c}_w(V, t = T)$, quantified over the regions V_{TOT}, V_{MBP}, V_{MBD} and V_{SB} from left to right, top to bottom.

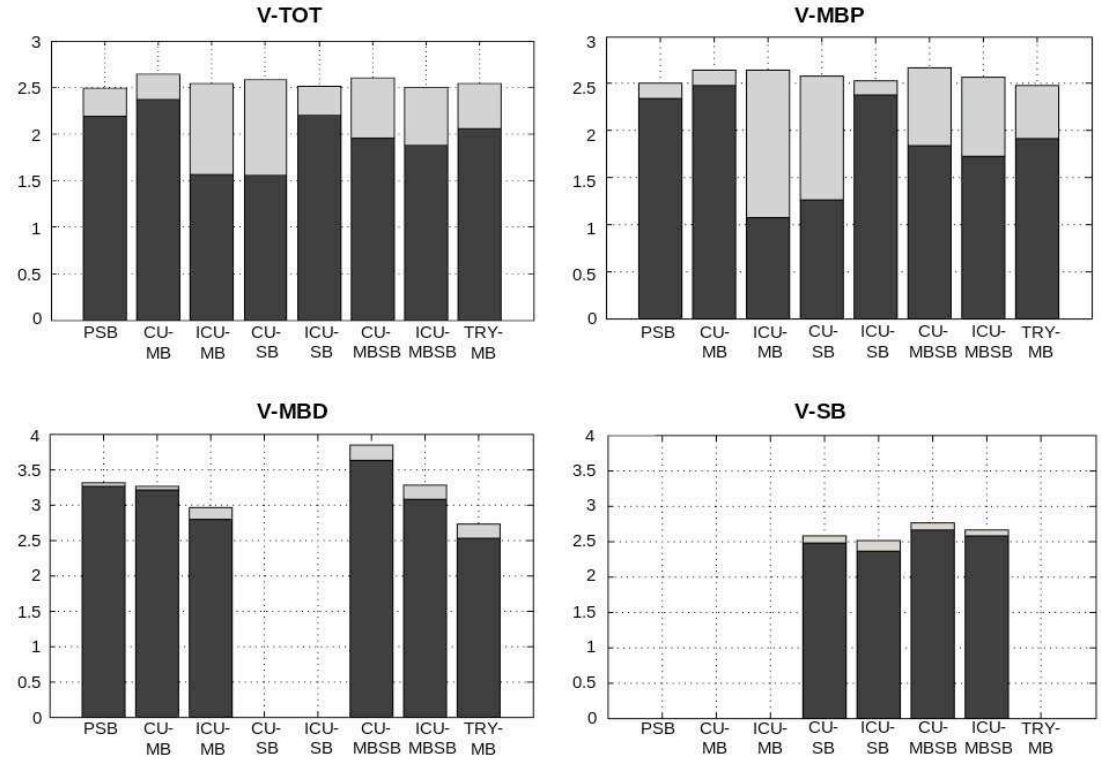

FIGURE 6: the normalized amount of delivered drug, namely, M_{eff} quantified over the regions V_{TOT}, V_{MBP}, V_{MBD} and V_{SB} from left to right, top to bottom.

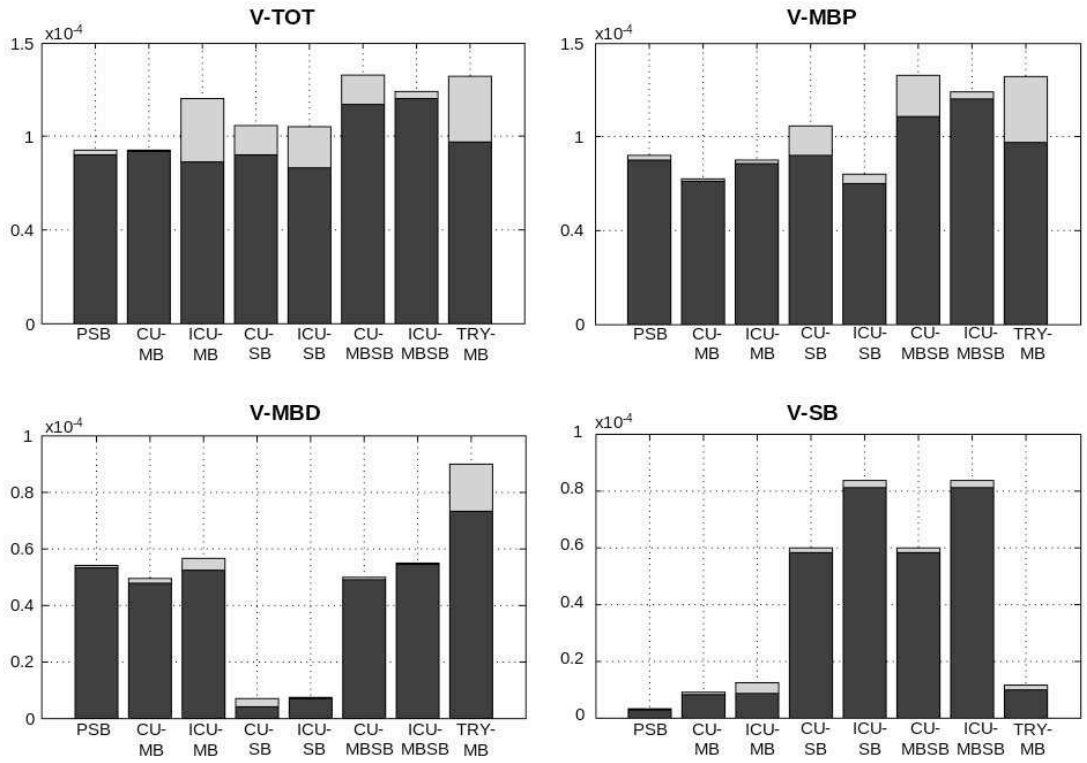

FIGURE 7: the maximum value of the dose $d_w^{\max}(V) = \max_{x \in V} d_w(x)$, quantified over the regions V_{TOT}, V_{MBP}, V_{MBD} and V_{SB} from left to right, top to bottom.

For each test, we report the total amount of drug delivered to V_{TOT}, V_{MBP}, V_{MBD} and V_{SB}. The amount of delivered drug is quantified by means of bars for both the incomplete and idealized apposition cases. Their differences are visualized superposing the increment corresponding to the idealized case upon each bar relative to the real configuration. The concentration scale refers to non-dimensional concentration units relative to $\bar{c}$, that is the saturation level of dissolved drug in water. The histograms in Fig 4 and 5 show the mean values of dose and drug concentration, $\bar{d}_w(V)$ and $\bar{c}_w(V, t = T)$ respectively, in different control volumes within the arterial wall. Since the dose quantifies the drug accumulation over time and the drug release profile behaves as $\sqrt{t}$, plots of mean values of drug concentration and dose are similar.

One-stent versus two-stent implantation: effect of drug delivery in the SB

One-stent and two-stent procedures are compared in order to evaluate the adequacy of the one-stent procedure in delivering drug to the SB. The main difference between these cases is that, in a one-stent procedure, the drug delivery to the SB is mainly achieved by flow mediated drug transport. On the other hand, if two DESs are implanted in both branches, drug is delivered through contact with the arterial wall, too. Moreover, minor variations could also depend on the fact that each stenting procedure deforms the vascular district differently and results in different local hemodynamic conditions. The influence of arterial deformation is evaluated (despite of other factors) by comparing the one-stent procedure with the CU and ICU techniques where only the stent in the MB is pharmacologically active. The comparison of tests PSB, CU-MB, ICU-MB with CU-MBSB and ICU-MBSB in Fig. 4 suggests that to achieve a more effective delivery in the artery, the implantation of two DES is mandatory. More precisely, for all stenting techniques, if the SB is treated with a BMS, drug delivered to the MB hardly

reaches the SB. Drug convection from the MB to the SB, which explains the amount of drug accumulated in the SB treated by a BMS, does not deliver a significant dosage in that area. Similar conclusions hold true for the control volume located at the distal part of the MB, namely V_{MBD}. If the CU or ICU procedures are performed by implanting a DES in the SB solely, then luminal drug transport would not be sufficient to adequately treat the arterial wall distal to the bifurcation.
Finally, in Fig. 7 the peaks of dose occurring within the entire artery as well as the local peaks relative to each control volume V_{MBP}, V_{MBD} and V_{SB} are reported. Peaks of dosage are rather uniformly distributed in the artery, with a small variability from region to region. In our view, this happens because local drug distribution depends on the stent pattern, i.e. on the local configuration of struts. Since the unit stent cell is periodically repeated along the artery, similar peaks of drug accumulation are observed, while stent implantation procedure and strut superposition barely affect maximal drug dosage.

Effects of stent overlap and struts apposition to the arterial wall
Each stent implantation technique is characterized by different contact surfaces between the stent and the artery and this factor highly affects the drug release. In particular, culotte techniques are characterized by a wide region in the proximal part of the MB where the two implanted devices overlap. Its influence on drug elution can be extracted from Fig. 4 and 6, in particular from the incremental part of the bar plots, which quantify the difference between the case of idealized apposition with respect to the realistic configuration.
In the one-stent case the drug loss due to incomplete strut apposition is the smallest, meaning that stent is almost completely apposed to the arterial wall. On the other hand, considerable losses take place when multiple stents are implanted. In particular, more than the 50% of the drug delivered by the superposed DES is lost in the blood stream and does not significantly contribute to healing the arterial wall. This finding is visible looking at incremental bars of cases CU-SB and ICU-MB where the active DES is obstructed by the superposition of another device between the DES and the artery. Conversely, CU-MB and ICU-SB, characterized by a direct contact between the DES and the artery, seem to be satisfactory. These conclusions are also confirmed by the comparison in Fig. 8 of the dose contour plots for ICU-MB in the case of incomplete and idealized strut apposition.

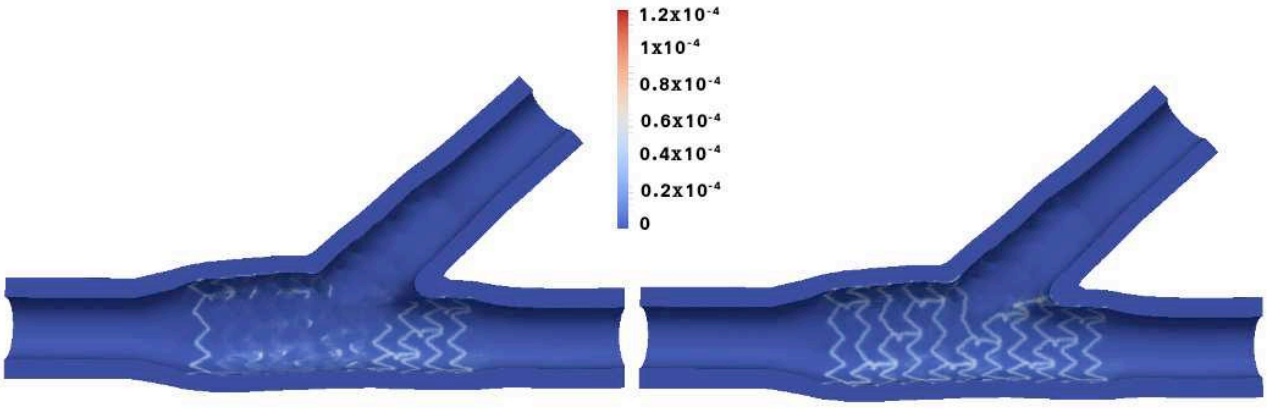

Figure 8: Dose contour plots for ICU-MB with realistic (left) and idealized strut apposition (right). The effect of strut superposition in limiting drug penetration into the arterial wall is clearly visible in the proximal part of MB where the two stents overlap.

The limitation of drug penetration into the arterial wall due to strut superposition is evident on the left. Another interesting evidence found is that average dosage in the whole artery in case of two DES

implanted is not doubled but it is only about 3/2 larger than in the case of one DES implantation into the MB. Due to stent superposition, a significant part of the drug charge is washed out in the blood stream. Furthermore, observing the amount of drug delivered to the entire vascular district, we notice that Culotte and Inverted Culotte techniques are almost equivalent, while some differences appear in the delivery to different sub-regions in the artery. The direct dependence of active surface of release with dosage is more accurately verified for ideal strut apposition than for the real case.
Similar conclusions are also confirmed by Fig. 6, reporting the normalized amount of delivered drug with respect to active surface of delivery, namely M_{eff} for t=T. Looking at the bars quantifying the release in the entire arterial wall for the ideal strut apposition, we notice that the effectiveness of delivery is almost equivalent in all cases, suggesting that strut apposition is the most important factor to ensure a good delivery. Respect to this variable, the best delivery performance is achieved for configurations PSB, CU-MB, ICU-SB, because there are no obstacles between the struts and the arterial wall. As expected, the configuration with two active stents (CU-MBSB and ICU-MBSB) are slightly penalized because the latter DES is superposed to the former. Clearly, CU-SB and ICU-MB cases are not efficient. Moreover, idealized efficiency of release is quantified around the value 2.5 in the regions V_{TOT}, V_{MBP} and V_{SB}, while it is slightly higher in the distal part of the MB (plot V_{MBD}) where it reaches values above 3.0. This effect may be due to the fact that part of the drug delivered to this region comes from drug washed out by blood flow from struts located upstream.

Use of dedicated stents for bifurcations

The comparison of cases ICU-MB and TRY-MB allows us to evaluate the performance of a dedicated stent to bifurcations and it highlights that this new approach might lead to some improvements in drug delivery. Its dedicated design, characterized by a lower metal density, guarantees a better apposition of the stent implanted in the MB and, consequently, a more effective drug delivery. Indeed, figure 4, 5 and 6 show a higher difference between the real and the idealized configurations in the ICU-MB case with respect to the TRY-MB case when evaluated in the proximal part of the MB. It means that the drug losses due to the stents superposition is minimized by the use of dedicated stent thanks to its design and the lower surface area in V_{MBP}. The different performance of the two configurations is also highlighted by Fig. 9 showing the drug distribution in the arterial wall for ICU-MB and TRY-MB cases. When compared to the CU technique, i.e. CU-MB case, Tryton stent slightly improves drug delivery to the distal part of the MB as well as to the SB (see Fig. 4, V_{MBD} and V_{SB} plots, respectively).

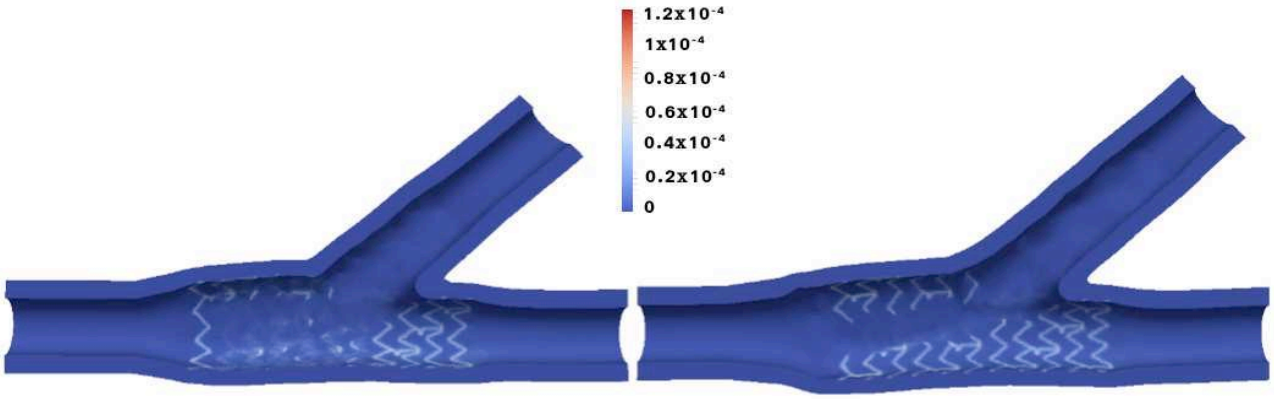

FIGURE 9: Dose contour plots for ICU-MB (right) and TRY-MB (left) with realistic strut apposition. The effect of a more uniform drug distribution is clearly visible for TRY-MB in the proximal part of MB.

Limitations

All the aforementioned results are based on the computational DES model, which is subject to some limitations. First, modeling inaccuracies account for the fact that the DES model or the parameters selected to characterize the different DES platforms may not exactly represent the reality. We do not have control on these errors, but at least we know that they equivalently affect all the considered test cases. As a result of that, we claim that any comparative conclusion is affected by the same error. On the contrary, quantitative values are highly sensitive to the modeling inaccuracies. For this reason, we are not claiming conclusions on the absolute scale of the results.

Lastly, all the simulations are performed to the highest accuracy allowed by the computational facility, which consists on a workstation equipped with a single Intel(R) Core(TM) i5 CPU 650 @ 3.20GHz and 4GB Ram. The sensitivity of the results with respect to the computational mesh have been investigated, confirming that numerical approximation errors do not significantly affect the reported results.

Conclusions

Computational modeling influences at multiple levels the design pathway of biomedical devices such as DES. First of all, it facilitates the mechanistic understanding of the significant phenomena at the basis of good device performance. A remarkable example for DES is provided by the sequel of papers [17,18,33,34] illustrating the interactions between drug release, intravascular drug metabolism and luminal flow patterns in determining arterial drug deposition. The present work stems from these models with the objective to upgrade the impact of computational modeling to the comparison of alternative clinical stenting protocols (such as PSB, CU or ICU). To succeed in this aim, it is mandatory to complement the aforementioned models for drug release, transport and absorption, with a realistic geometrical description of the devices and their deformations induced during stenting. By this way, we are able to study the inhomogeneity of drug delivery to a realistic bifurcating coronary model, or to quantify how much stent superposition affects drug losses in the blood stream. We hope these results may stimulate further research on the design of dedicated stents to arterial bifurcations and may help to refine guidelines to prescribe one or another stenting protocol to specific patients. The final stage of computational models applied to biomedical devices consists in providing reliable quantitative results, which, unfortunately, is far from being reached yet.

Acknowledgments: All the authors have been supported by the Grant Nanobiotechnology: Models and methods for degradable materials of the Italian Institute of Technology (IIT). The authors E. Cutri' and P. Zunino are also supported by the European Research Council Advanced Grant Mathcard, Mathematical Modelling and Simulation of the Cardiovascular System, Project ERC-2008-AdG 227058. Francesco Migliavacca, Stefano Morlacchi and Claudio Chiastra are partially supported by the project “RT3S- Real Time Simulation for Safer vascular Stenting” funded by the European Commission under the 7th Framework Programme, GA FP7-2009-ICT-4-248801.

References

1. A.R. Assali, H.V. Assa, I. Ben-Dor, I. Teplitsky, A. Solodky , D. Brosh, S. Fuchs, R. Kornowski, Drug-Eluting Stents in Bifurcation Lesions: To Stent One Branch or Both?, Catheter. Cardiovasc. Interv. 68 (2006) 891–896.
2. T. Lefévre, Y. Louvard, M.C. Morice, P. Dumas, C. Loubeyre, A. Benslimane, R.K. Premchand, N. Guillard, J.F. Piechaud, Stenting of bifurcation lesions: classification,

treatments, and results, Catheter. Cardiovasc. Interv. 49 (2000) 274–283.
3. I. Iakovou, L. Ge, A. Colombo, Contemporary Stent Treatment of Coronary Bifurcations, J. Am. Coll. Cardiol. 46 (2005) 1446-1455.
4. M. Pan, J. Suárez de Lezo, A. Medina, M. Romero, J. Segura, A. Ramírez, D. Pavlovic, E. Hernández, S. Ojeda, C. Adamuz, A stepwise strategy for the stent treatment of bifurcated coronary lesions, Catheter. Cardiovasc. Interv. 55 (1) (2002) 50-7.
5. Hoye, A., Contemporary percutaneous coronary intervention for complex lesions: the treatment of chronic total occlusions and bifurcationsin the drug-eluting stent era, Ph.D. Thesis, 2006 , http://repub.eur.nl/res/pub/7642/
6. M.C. Morice, P.W. Serruys, J.E. Sousa, J. Fajadet, E. Ban Hayashi, M. Perin, A. Colombo, G. Schuler, P. Barragan, G. Guagliumi, F. Molnàr, R. Falotico, A randomized comparison of a sirolimus-eluting stent with a standard stent for coronary revascularization, N. Engl. J. Med. 346 (2002) 1773–1780.
7. S.J. Park, D.W. Park, Left main stenting: is it a different animal, EuroIntervention 6 (2010) J112-J117.
8. M.A. Lovich, E.R. Edelman, Computational simulations of local vascular heparin deposition and distribution, Am. J. Physiol. Heart Circ. Physiol. 271 (1996) H2014–H2024.
9. G. Pontrelli, F. de Monte, A multi-layer porous wall model for coronary drug-eluting stents, Int J Heat Mass Transf, 53 (2010) 3629-3637.
10. C.W. Hwang, D. Wu, E.R. Edelman, Physiological transport forces govern drug distribution for stent-based delivery, Circulation 104 (5) (2001) 600–605.
11. P. Zunino, Multidimensional pharmacokinetic models applied to the design of drug-eluting stents, in: Cardiovascular Engineering 4,181–191.2004.
12. M. Grassi, G. Pontrelli, L. Teresi, G. Grassi, L. Comel, A. Ferluga, L. Galasso, Novel design of drug delivery in stented arteries: a numerical comparative study, Math. Biosci. Eng. 6 (3) (2009) 493–508.
13. G. Vairo, M. Cioffi, R. Cottone, G. Dubini, F. Migliavacca, Drug release from coronary eluting stents: A multidomain approach, J. Biomech. 43 (2010) 1580–1589.
14. D.R. Hose, A.J. Narracott, B. Griffiths, S. Mahmood, J. Gunn, D. Sweeney, P.V. Lawford, A thermal analogy for modelling drug elution from cardiovascular stents, Comput. Methods Biomech. Biomed. Engin. 7 (2004), 257–264.
15. F. Migliavacca, F. Gervaso, M. Prosi, P. Zunino, S. Minisini, L. Formaggia, G. Dubini, Expansion and drug elution model of a coronary stent, Comput. Methods Biomech. Biomed. Engin. 10 (2007) 63–73.
16. P. Zunino, C. D'Angelo, L. Petrini, C. Vergara, C. Capelli, F. Migliavacca, Numerical simulation of drug eluting coronary stents: Mechanics, fluid dynamics and drug release, Comput. Methods Appl. Mech. Engrg. 198 (2009) 3633–3644.
17. B. Balakrishnan, A.R. Tzafriri, P. Seifert, A. Groothuis, C. Rogers, E.R. Edelman, Strut position, blood flow, and drug deposition, implications for single and overlapping drug-eluting stents, Circulation 111 (2005) 2958–2965.
18. B. Balakrishnan, J.F. Dooley, G. Kopia, E.R. Edelman, Intravascular drug release kinetics dictate arterial drug deposition, retention, and distribution, J. Control. Release 123 (2) (2007) 100–108.
19. B. Balakrishnan, J.F. Dooley, G. Kopia, E.R. Edelman, Thrombus causes fluctuations in arterial drug delivery from intravascular stents, J. Control. Release 131 (2008) 173–180.
20. R. Mongrain, R. Leask, J. Brunette, I. Faik, N. Bulman-Feleming, T. Nguyen, Numerical modeling of coronary drug eluting stents, Stud. Health Technol. Inform. 113 (2005) 443–458.
21. R. Mongrain, I. Faik, R.L. Leask, J. Rodés-Cabau, E. Larose, O.F. Bertrand, Effects of

diffusion coefficients and struts apposition using numerical simulations for drug eluting coronary stents, J. Biomech. Eng. 129 (2007) 733–742.
22. A. Borghi, E. Foa, R. Balossino, F. Migliavacca, G. Dubini, Modelling drug elution from stents: effects of reversible binding in the vascular wall and degradable polymeric matrix, Comput. Methods Biomech. Biomed. Engin. 11 (2008) 367–377.
23. B. Chevalier, B. Glatt, T. Royer, P. Guyon, Placement of coronary stents in bifurcation lesions by the "culotte" technique, Am. J. Cardiol. 82 (8) (1998) 943-9.
24. T. Adriaenssens, R.A. Byrne, A. Dibra, R. Iijima, J. Mehilli, O. Bruskina, A. Schomig, A. Kastrati, Culotte stenting technique in coronary bifurcation disease: angiographic follow-up using dedicated quantitative coronary angiographic analysis and 12-month clinical outcomes, Eur. Heart J. 29 (2008) 2868–2876.
25. G. Stankovic, Z. Mehmedbegovic, M. Zivkovic, Bifurcation Coronary Lesions – Approaches to Bifurcation Management, J. Interv. Cardiol. 5 (2010) 53–7.
26. C. D'Angelo, P. Zunino, Robust Numerical approximation of the coupled Stokes' and Darcy's flows applied to vascular hemodynamics and biochemical transport ESAIM: M2AN 45 (2011) 447–476.
27. C. D'Angelo, P. Zunino, Numerical approximation with Nitsche's coupling of transient Stokes'/Darcy's flow problems applied to hemodynamics, Applied Numerical Mathematics, in press
28. C. D'Angelo, P. Zunino, A. Porpora, S. Morlacchi, F. Migliavacca, Model reduction strategies enable computational analysis of controlled drug release from cardiovascular stents, To appear in SIAM J. Appl. Math., 2012.
29. D. Gastaldi, S. Morlacchi, R. Nichetti, C. Capelli, G. Dubini, L. Petrini, F. Migliavacca, Modelling of the provisional side-branch stenting approach for the treatment of atherosclerotic coronary bifurcations: effects of stent positioning, Biomech. Model. Mechanobiol. 9 (2010) 551- 561.
30. S. Morlacchi, C. Chiastra, D. Gastaldi, G. Pennati, G. Dubini, F. Migliavacca, Sequential Structural and Fluid Dynamic Numerical Simulations of a Stented Bifurcated Coronary Artery, J. Biomech. Eng. 133 (2011), 121010.
31. G. Frenning, Theoretical investigation of drug release from planar matrix systems: effects of a finite dissolution rate, J. Control. Release 92 (2003) 331-339.
32. P. Biscari, S. Minisini, D. Pierotti, G. Verzini, P. Zunino, Controlled release with finite dissolution rate, SIAM J. Appl. Math. 71 (2011) 731–752.
33. V.B. Kolachalama, A.R. Tzafriri, D.Y. Arifin, E.R. Edelman, Luminal flow patterns dictate arterial drug deposition in stent-based delivery, J. Control. Release 133 (2009) 24–30.
34. V.B. Kolachalama, E.G. Levine, E.R. Edelman, Luminal flow amplifies stent-based drug deposition in arterial bifurcations, PLoS One. 4 (12) (2009) e8105 1-9.
35. K. Perktold, M. Hofer, G. Rappitsch, M. Loew, B.D. Kuban, M.H. Friedman, Validated computation of physiologic flow in a realistic coronary branch, J Biomech, 31 (1998), 217-228.
36. R. Tzafriri, A.D. Levin, E.R. Edelman, Diffusion-limited binding explains binary dose response for local arterial and tumour drug delivery, Cell Prolif. 42 (2009) 348–363.
37. D.V. Sakharov, L.V. Kalachev, D.C. Rijken, Numerical simulation of local pharmacokinetics of a drug after intravascular delivery with an eluting stent, J. Drug Targ. 10 (2002) 507-513.
38. T. Higuchi, Rate of release of medicaments from ointment bases containing drugs in suspension, J. Pharm. Sci. 50 (1961) 874-875.
39. M.A. Lovich, E.R. Edelman, Computational simulations of local vascular heparin deposition and distribution, Am. J. Physiol. Heart Circ. Physiol. 271 (1996) 214-224.
40. I. Sheiban, G. Villata, M. Bollati, D. Sillano, M. Lotrionte, G. Biondi-Zoccai, Next-generation

drug-eluting stents in coronary artery disease: focus on everolimus-eluting stent (Xience V®), Vasc. Health Risk Manag. 4 (1) (2008) 31-38.
41. C. Collet, R.A. Costa, A. Abizaid, Dedicated bifurcation analysis: dedicated devices, Int. J. Cardiovasc. Imaging 27 (2011) 181-188.

MOX Technical Reports, last issues

Dipartimento di Matematica "F. Brioschi",
Politecnico di Milano, Via Bonardi 9 - 20133 Milano (Italy)

16/2012 Cutr, E.; Zunino, P.; Morlacchi, S.; Chiastra, C.; Migliavacca, F.
Drug delivery patterns for different stenting techniques in coronary bifurcations: a comparative computational study

15/2012 Mengaldo, G.; Tricerri, P.; Crosetto,P.; Deparis, S.; Nobile, F.; Formaggia, L.
A comparative study of different nonlinear hyperelastic isotropic arterial wall models in patient-specific vascular flow simulations in the aortic arch

14/2012 Fumagalli, A.;Scotti, A.
An unfitted method for two-phase flow in fractured porous media.

13/2012 Formaggia, L.; Guadagnini, A.; Imperiali, I.; Lever, V.; Porta, G.; Riva, M.; Scotti, A.; Tamellini, L.
Global Sensitivity Analysis through Polynomial Chaos Expansion of a basin-scale geochemical compaction model

12/2012 Guglielmi, A.; Ieva, F.; Paganoni, A.M.; Ruggeri, F.
Hospital clustering in the treatment of acute myocardial infarction patients via a Bayesian semiparametric approach

11/2012 Bonnemain, J.; Faggiano, E.; Quarteroni A.; Deparis S.
A Patient-Specific Framework for the Analysis of the Haemodynamics in Patients with Ventricular Assist Device

10/2012 Lassila, T.; Manzoni, A.; Quarteroni, A.; Rozza, G.
Boundary control and shape optimization for the robust design of bypass anastomoses under uncertainty

09/2012 Mauri, L.; Perotto, S.; Veneziani, A.
Adaptive geometrical multiscale modeling for hydrodynamic problems

08/2012 Sangalli, L.M.; Ramsay, J.O.; Ramsay, T.O.
Spatial Spline Regression Models

07/2012 Perotto, S; Zilio, A.
Hierarchical model reduction: three different approaches